ELSEVIER

Biochimica et Biophysica Acta 1187 (1994) 99–105

BBA Biochimica et Biophysica Acta

Structure of Photosystem I: Suggestions on the docking sites for plastocyanin, ferredoxin and the coordination of P700

Petra Fromme [a,*], Wolf-Dieter Schubert [b], Norbert Krauß [b]

[a] *Max-Volmer Institut für Biophysikalische und Physikalische Chemie, Technische Universität Berlin, Straße des 17. Juni 135, 10623 Berlin, Germany,* [b] *Institut für Kristallographie, Freie Universität Berlin, Takustraße 6, 14195 Berlin, Germany*

Received 10 March 1994

Abstract

Photosystem I of *Synechococcus elongatus* was crystallized showing maximal diffraction to 4 Å resolution (Witt et al. (1988) Ber. Bunsenges. Phys. Chem. 92, 1503–1506). The crystal structure has been determined at a resolution of 6 Å (Krauß et al. (1993) Nature 361, 326–331). Based on this structure, docking sites for plastocyanin and ferredoxin are proposed. The arrangement of helices is analysed in terms of hydrophobicity plots and homology to the reaction center of purple bacteria. A possible coordination of the primary donor P700 by the helices in subunits A and B is suggested based on the relative three-dimensional arrangement of the helices.

Key words: Photosystem I; Crystal; X-ray structure; Photosynthesis; Plastocyanin; Ferredoxin

1. Introduction

The first step of photosynthesis is the light induced charge separation followed by the directed electron transport across the photosynthetic membrane. In higher plants and cyanobacteria this takes place within two membrane-integral protein complexes, the Photosystems I and II. Photosystem II utilizes water as electron donor, and shows similarities in respect of amino acid sequence and composition of electron transport carriers to the bacterial reaction center (b-RC) of purple bacteria, despite this reaction center being unable to use water as electron donor. The structure of the reaction center of purple bacteria has been determined by X-ray diffraction methods [1,2].

By comparison, Photosystem I shows nearly no primary sequence homology and significant differences in the composition and arrangement of electron carriers. In contrast to Photosystem II about 90 antenna chlorophyll molecules are bound by the large subunits A and B of PS I. These subunits also carry the primary donor P700 (probably a chlorophyll *a* dimer, the first electron acceptor A0 (chlorophyll *a*), the second electron acceptor A1 (vitamin K1) and the first 4Fe-4S cluster F_x. The two terminal iron-sulfur clusters F_A and F_B are bound to the small stromal subunit C. From the terminal iron-sulfur cluster the electron is transferred to the soluble ferredoxin, which carries it to the NADP reductase (for review see [3]). At the lumenal side, $P700^+$ is re-reduced by plastocyanin. In the case of cyanobacteria cytochrome c_6 may also be used as alternative electron donor.

2. Progress in characterization and crystallization of Photosystem I

Photosystem I from the thermophilic cyanobacterium *Synechococcus sp.*, now reclassified as *Synechococcus elongatus* [4], was characterized by isolation and sequencing of the genes of 11 subunits: the two large subunits A and B; three subunits (C, D and E) located on the stromal side; the subunit F, located at the lumenal side of Photosystem I; and five small membrane intrinsic subunits named I, J, K, L and M [5]. The presence of subunit L and I in the crystals

Abbreviations: PS I, Photosystem I; PS II, Photosystem II; Chl *a*, chlorophyll *a*; b-RC, reaction center of purple bacteria; Cyt c_6, cytochrome c_6

* Corresponding author. Fax: +49 30 31421122.

SSDI 0005-2728(94)00079-K

could previously not be ascertained, but subunit L has now been identified in the crystals by peptide specific antibodies (Haehnel, W., personal communication).

Photosystem I was isolated from the membrane in a trimeric form and there is evidence that the trimer also exists in the native membrane [6,7]. The molecular mass of the Photosystem I monomer [8] has been estimated to be 340 kDa on the basis of the subunit composition and the chlorophyll content; i.e., about 1 MDa in the case of the trimer.

The Photosystem I trimer was crystallized by dialysis against low salt concentration of $MgSO_4$. After 1 or 2 days, dark-green hexagonal prisms, either elongated, needle-shaped or plate-like are obtained. The crystals diffract to a resolution of 4 Å [9,10]. Data sets were initially measured to a resolution of 6 Å using synchrotron X-radiation and the structure of Photosystem I was determined [11]. To date, we have collected a native data set of 3.8 Å resolution and several heavy atom derivative data sets at 4 to 4.5 Å resolution. The evaluation of a number of data sets is in progress, but even based on the structure at 6 Å further information can be inferred about the possible docking sites for ferredoxin, plastocyanin and the coordination of P700.

2.1. Structure of Photosystem I

Based on the 6 Å map [11], 28 tubular structures interpreted as alpha-helices were identified. Out of these 21 are transmembrane. They are depicted in Fig. 1A as seen from the stromal side. 16 of these helices (in grey in Fig. 1A) are structurally related to each other by local two-fold symmetry. The axis of this non-crystallographic two-fold symmetry passes through the iron-sulfur cluster F_X. Two 'horizontal' helices n and n′ at the lumenal side also obey this two-fold symmetry. The 16 transmembrane helices and the two helices parallel to the membrane plane were assigned to the large subunits A and B.

40 of the 90 antenna chlorophylls have been located. They are oriented nearly perpendicular to the membrane plane and grouped to surround the inner ring of helices.

The position of the three iron-sulfur clusters could be inferred from dense peaks of electron density on the stromal side of PSI. Between F_x and the lumenal surface of the protein electron density features were interpreted as the carriers of the electron transport chain (Fig 1B): P700, two additional chl *a* in the vicinity of P700, A0 and, rather speculatively, A1.

Comparing this structure with the present knowledge of PSI from molecular biological, biophysical and biochemical investigations some interesting questions arise:

(a) Where are the most reasonable docking sites for the soluble electron carriers plastocyanin (or cytochrome c_6) on the lumenal side and for ferrodoxin on the stromal side of Photosystem I?

(b) Hydrophobicity plots (Fig. 1C Kyte & Doolittle) of the large subunits A and B indicated 10–12 transmembrane helices for each. Only 8 transmembrane helices were, however, identified in the electron density map. Furthermore the electron density reveals two helices running parallel to the membrane plane near the lumenal indentation near the primary donor P700. These were not predicted, previously, but presumably belong to the large subunits A and B, due to their symmetry relation.

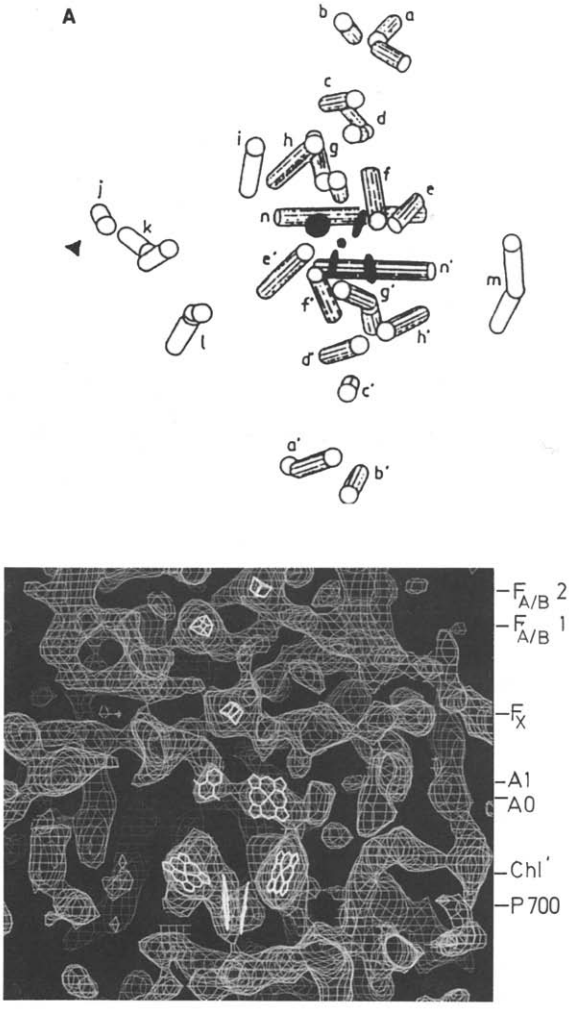

Fig. 1. (A) view from the stromal side of Photosystem I onto the membrane plane. The assigned helices are shown as columns. The transmembrane helices are shown as well as two 'horizontal helices' at the lumenal side of Photosystem I. The chlorophylls of P700 and the accessory chlorophylls are represented by discs. The helices, shown in grey are structurally related to each other by a local twofold dyad, passing through the iron-sulfur center F_x, and are therefore assigned to the large subunits A and B. (from [10]) (B) Part of the electron density map between $F_{A/B}$ 2 and the lumenal surface. Electron densities are interpreted as carriers of the electron transport chain. (from [11]) (C) Hydrophobicity plot (Kyte and Doolittle) of the large subunits A and B. (From Ref. [27].)

(c) Which of the helices, surrounding the electron transfer chain, can most reasonably be assumed to be involved in the coordination of the primary donor P700?

2.2. Docking site for plastocyanin or cytochrome c_6

It was shown [12] that plastocyanin can be crosslinked to subunit F in spinach, suggesting the direct binding of plastocyanin to this subunit. New results on mutants of *Synechocystis PCC 6803* lacking subunit F [13] show that photoautotrophic growth was not influenced by this deletion. Furthermore, the kinetics of electron transfer from cytochrome c_6 to P700 were not influenced by the removal of subunit F by detergent in *Synechoccus elongatus* [14]. It therefore appears that plastocyanin and cytochrome c_6 interact directly with the large subunits A and B. The most

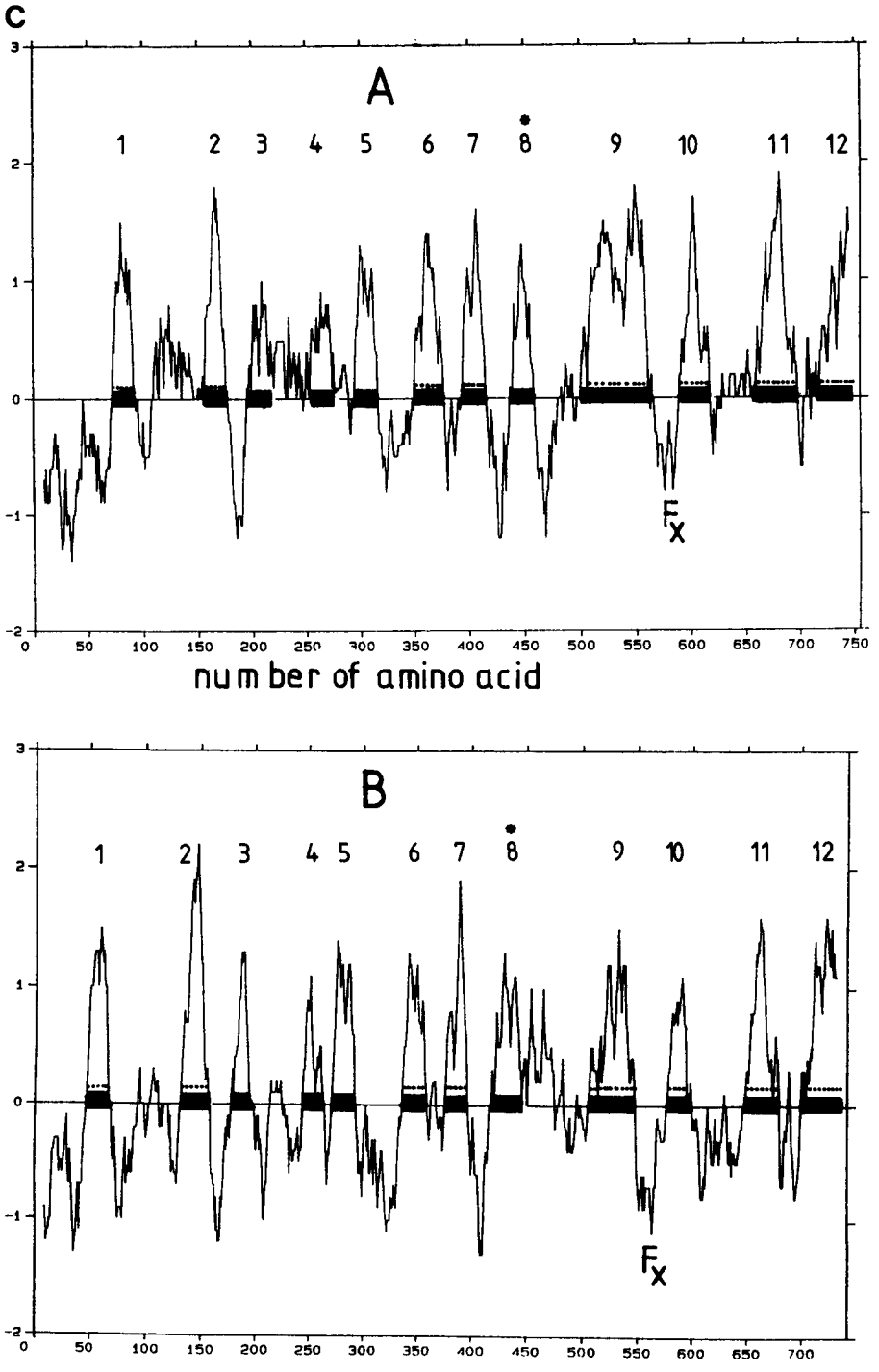

Fig. 1 (continued).

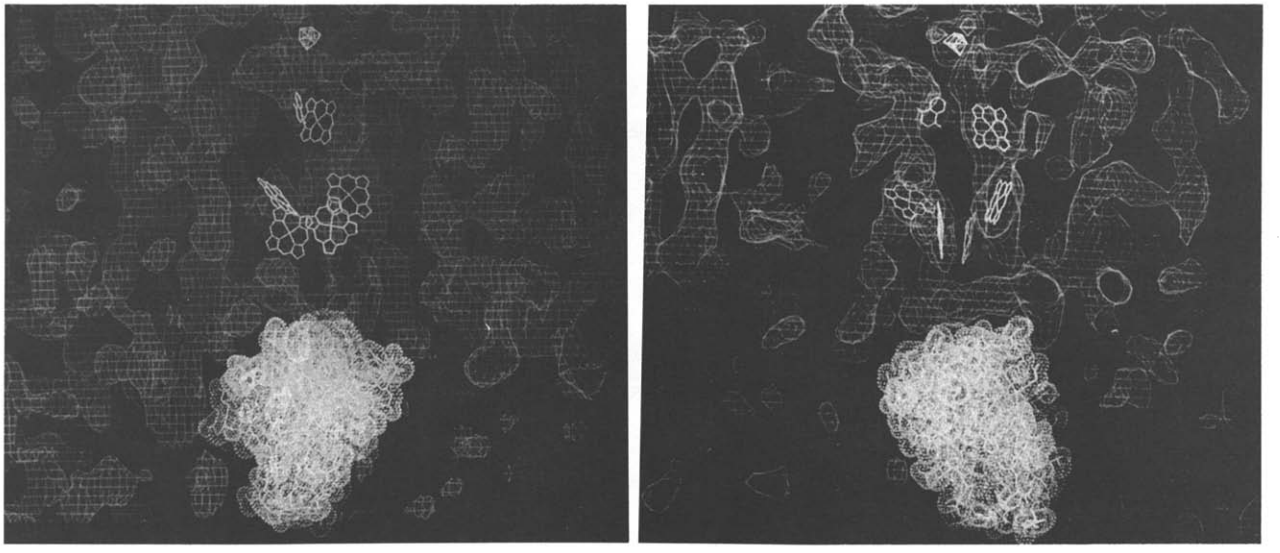

Fig. 2. Electron density map of Photosystem I including the structure of plastocyanin from *Enteromorpha prolifera* [15] in its proposed docking site. Seven assigned molecules of the electron transfer chain (F_x to P700) are also shown for added clarity. Plastocyanin is depicted with its Van der Waals surface. Left side: view along the membrane plane. Right side: rotated to the left side by a rotation of ≈ 90° around the vertical axis.

feasible binding site for plastocyanin is inside an indentation on the lumenal side of PSI, near the two 'horizontal' helices n and n'. Fig. 2 shows this part of the electron density with the structure of plastocyanin from *Enteromorpha prolifera* (green alga) [15] (Brookhaven data bank entry 7PCY) modelled inside the cavity. The distance from Cu^{2+} to the center of the chlorophylls of P700 is about 20 Å. As may be seen, the dimensions of plastocyanin match this cavity well. It should be noted that in cyanobacteria cytochrome c_6 can be used as alternative electron donor. The structure of this cytochrome has not been solved as yet, but the size of the two proteins is comparable as judged by their amino acid sequence.

2.3. Docking site for ferredoxin

The positions of the three iron-sulfur clusters were identified unambiguously as peaks of electron density

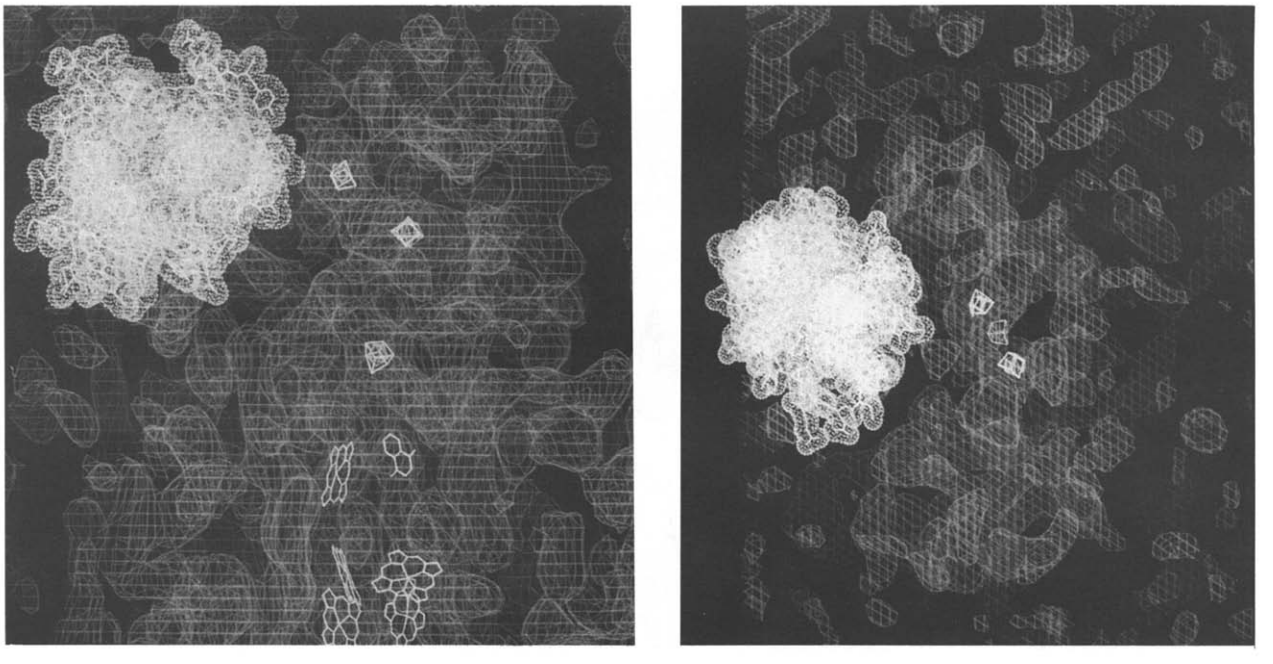

Fig. 3. Electron density map of Photosystem I fitted with ferredoxin from *Spirolina platensis* [16], incorporated in its modelled orientation. In addition the nine assigned molecules of the electron transfer chain (P700 to $F_{A/B}$) are shown. Ferredoxin is depicted with its Van der Waals surface. Left side: view along the membrane plane. Right side: view from the stromal side onto the membrane plane.

significantly above the mean density of the protein. The organization of the three clusters suggests an unidirectional electron transport from F_x via the first terminal iron-sulfur cluster $F_{A/B}$ 1 (at a distance of 15 Å from F_x) to the second iron-sulfur cluster $F_{A/B}$ 2 (at a distance of 12 Å to $F_{A/B}$ 1 and 22 Å to F_x). The iron-sulfur center $F_{A/B}$ 1 is embedded deeply within the protein matrix, the shortest distance from the center of $F_{A/B}$ 1 to the surface of the protein being approx. 16 Å.

Near the second terminal iron-sulfur cluster, $F_{A/B}$ 2, a possible docking site for ferredoxin was identified. The distance from the center of $F_{A/B}$ 2 to the surface is about 12 Å for this site. Fig. 3 shows this region of the electron density map together with the structure of a soluble ferredoxin from *Spirulina platensis* [16], taken from the Brookhaven data bank entry 3FXC. The ferredoxin from our cyanobacterium is closely related to this ferredoxin, as deduced from sequence homology [17], and also binds a 2Fe-2S cluster. It is evident from Fig. 3 that ferredoxin fits this possible docking site well. The distance from the center of the iron-sulfur cluster $F_{A/B}$ 2 to the center of the 2Fe-2S cluster of the ferrodoxin is about 14 Å, which is suitable for rapid electron transfer [18]. It must be noted, however, that this distance is only an estimate, as experimental information on the orientation of ferredoxin is lacking and also because there may be some small structural differences between the ferredoxin of *Spirulina platensis* and that of *Synechococcus elongatus*.

A second electron transport route directly from the first iron-sulfur cluster $F_{A/B}$ 1 to ferredoxin, binding at an alternative site closer to $F_{A/B}$ 1 (on the right side of the stromal hump in Fig. 3), cannot be ruled out. This is, however, less likely because of the larger distance to the protein surface. Binding of ferredoxin to this second site will lead to a smallest center to center distance of about 19 Å between the iron-sulfur centers. Because electron transfer rates are inversely related to the distance between electron carriers [18], the kinetics of ferredoxin reduction at the second site must be significantly lower than that for the preferred binding site closer to $F_{A/B}$ 2.

2.4. Arrangement of helices

A clear discrepancy exists between the number of transmembrane helices in the large subunits A and B of Photosystem I as predicted on the basis of hydrophobicity plots of spinach [19] and maize [20] on the one hand and those actually identified in the electron density map (8 transmembral, 1 lumenal) on the other hand. The latter are illustrated in Fig. 1A in a view looking from the stromal side onto the membrane plane. A hydrophobicity plot based on the sequence of PsaA and PsaB from *Synechococcus elongatus* is shown in Fig. 1C [27]. In the past, various predictions for the arrangement of helices have been put forward:

– A structural model of the large subunits of Photosystem I based on the arrangement of helices in Photosystem II and purple bacteria RC, was formulated [21]. This model is not confirmed by the observed arrangement of helices:

In bacterial reaction centers the transmembane helices D and E of subunit L and M are situated in close proximity to the local dyad, and are in contact with each other [1,22]. By contrast, the transmembrane helices in Photosystem I surround the electron transfer chain like a fence. The number of 13 helices in the model can not be confirmed in the structure.

– A leucine zipper was proposed to be involved in the dimer formation of the two large subunits A and B [23]. Because the smallest distance between structurally related helices is 20 Å this possibility can be ruled out. This is consistent with mutation experiments on the corresponding leucine residues in *Synechocystis PCC 6803*, which have identical behavior to the wild type Photosystem I [24].

We suggest the following correlation between the 10–12 regions, proposed to represent transmembrane helices on the basis of hydrophobicity analysis (see Fig. 1C) and the 8 transmembrane helices + one 'horizontal' helix, observed in the structure at 6 Å:

The iron-sulfur center F_X is coordinated by 4 cysteins: Two from each of the large subunits A and B. Consequently, the binding site for the iron-sulfur center Fx may be deduced directly from the primary sequence. It is located between the predicted helices 9 and 10 in Fig. 1C. The four helices predicted to be at the C-terminus of the large subunits (9, 10, 11 and 12) are all confirmed using different hydrophobicity programs [25,26], (data not shown). They are all of sufficient length to span the membrane. Because they are close to the binding site of F_x we propose that the 4 helices surrounding the electron transfer chain should be assigned to the C-terminal region of the primary sequence and the N-terminal region of the protein in turn to be involved in the binding of antenna chlorophylls. Possibly, the evolutionary ancestor of the subunits A and B was formed by a gene fusion of a gene for a light harvesting protein and a gene for a photoreaction center.

The respective lengths of the symmetry related helices, surrounding the electron transfer chain (e, f, g, h, and e′, f′, g′, h′) are comparable in both subunits, except for helices g and g′ (see Fig 1A). The kinked helix g is the longest helix in the protein complex, with a length of 35 amino acids, whereas the corresponding helix g′ is significantly shorter, with 24 amino acids. Comparing this length to the amino acid sequence and the hydrophobicity plot (Fig. 1C), there is only one region with such a long hydrophobic sequence: the

proposed helix 9 in subunit A. This hydrophobic region is significantly shorter in subunit B. It should be noted that there is a proline in both sequences, which could explain the kink in the helices. On this basis, we propose that helix g belongs to subunit A and corresponds to the region of the helix 9 in the hydrophobicity plot. Helix g′ belongs to subunit B and belongs to the corresponding amino acid region. However, we do not imply, that all unprimed helices can similarly be assigned to subunit A and all primed helices belong to subunit B.

Some proposed helices in the N-terminal region of the protein (helices 3, 4 and 5) are of insufficient length to form a membrane spanning helix and/or are not predicted using improved hydrophobicity programs [24] (data not shown) and so it is reasonable that these hydrophobic regions do not form transmembrane helices.

A remarkable feature of the secondary structure is the existence of the 'horizontal' helices n and n′ which were not predicted previously, but which seem to play a prominent role in the structure of Photosystem I. They are located at the lumenal side, shielding P700 from the aqueous phase and are possibly involved in plastocyanin/cytochrome c_6 docking (see above). They are arranged symmetrically with respect to the two chlorophyll molecules of the primary donor P700. The shortest distance of the center of the chlorophylls to the middle of these helices is only 11 Å indicating that they may well be involved in the coordination of P700 or the 'accessory chlorophylls'.

The sequence homology between the correlated transmembrane regions of subunit A and B is about 45%, but for the region of the proposed helix 8 80% of the amino acid residues are identical. These helices are flanked by two regions which are rich in basic amino acids. A common motif H XX W XXX F occurs in both subunits, in which the three aromatic amino acids lie on one side of the helix, while the other side consists of aliphatic amino acids.

In the reaction center of purple bacteria two horizontal helices were also observed near the primary donor, in both L and M subunit, which contain the same consensus sequence H XX W XXX F. In fact, the X-ray structure [1,2] shows that these three aromatic amino acids are indeed located on one side of the helix with the histidine coordinating the Mg of one of the accessory chlorophylls.

Therefore we propose, that the region of the proposed hydrophobic region 8 can be assigned to the helices n and n′ (Krabben, Kuhn and Fromme in preparation). This result will have consequences for the proposed docking site for plastocyanin/cytochrome c_6:

The orientation of the helices n and n′ will be such, that the side with the aromatic amino acids is located close to P700, while the other, aliphatic side faces the lumenal surface of the protein, at the proposed docking site for plastocyanin. Consequently a hydrophobic surface, at the lumenal indentation is proposed for docking of plastocyanin/cytochrome c_6 (see Fig. 3, right). Thus we propose that the hydrophobic regions 1, 2, 6, 7 and 9, 10, 11, 12 (dotted in Fig. 1C) form the 8 transmembrane helices of subunits A and B, obtained in the electron density map; the hydrophobic regions 8 (marked with a star in Fig. 1C) form the lumenal 'horizontal' helices n and n′.

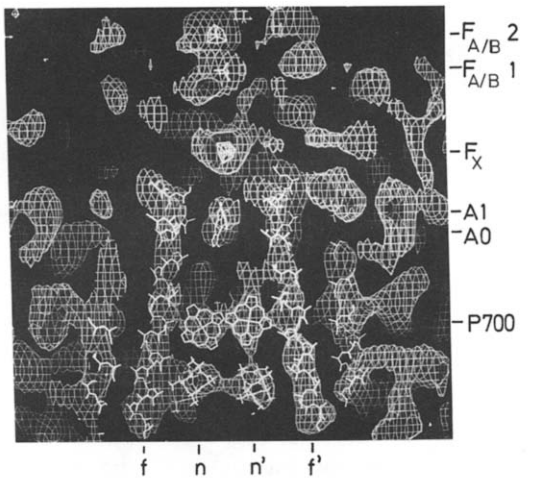

Fig. 4. Part of the electron density map with modelled polyalanine helices and dihydroporphyrine rings of chlorophylls from the electron transport chain between F_x and the lumenal surface. The two helices adjacent to P700 correspond to helices f and f′ in Fig. 1A. At the bottom of the figure, at the lumenal side, the two helices n and n′ are located.

2.5. Coordination of P700

As discussed previously, it appears reasonable that helices n and n′ may play a role in coordination of P700 and/or the 'accessory chlorophylls'. In addition, however, some of the transmembrane helices would be expected to participate in the coordination of P700. Fig. 4 shows a detailed view of the electron density surrounding P700. The electron density attributed to P700 forms the center, flanked on either side by the two helices f and f′, while n and n′ are located at the lumenal side. The distance from the center of each chlorophyll to the center of the helices is 7–8 Å. The helices g and g′, are at a distance of at least 13 Å to the center of these chlorophylls).

Helices e and e′ are also in close proximity to the chlorophylls of P700. The shortest distance from the center of the chlorophylls to the center of the helices e and e′ is 7–8 Å, as is the case for the helices f and f′. Relative to Fig. 4, e is located behind the chlorophyll on the left side, while e′ is in front of the chlorophyll

on the right side (see also Fig. 1A). The angles between the axes of both helices e and e′ and the membrane normal are about 30°. Comparing the arrangement of helices to the coordination of the primary donor in the bacterial reaction center, which is coordinated by histidine from helices LD and MD to the Mg^{2+} of the chlorophylls, there are similarities to the arrangement of e and e′ to the chlorophylls of P700.

On the other hand, it is also possible, that the helices f and f′ coordinate the primary donor P700. In both cases the coordinating amino acid, which is proposed to be a histidine, must be located between amino acids 10 and 13 as counted from the lumenal side. The hydrophobic region 11 does indeed contain one histidine, which is near the middle of the hydrophobic sequence. This histidine H685 of subunit A forms part of the motif LAGHF XXX F. A corresponding sequence occurs in the M-subunit of the bacterial reaction center, where the H202 in *Rhodospeudomonas sphaeroides*, which coordinates one chlorophyll of the special pair, is surrounded by the sequence F XXX FHGL. The same motif is also found in subunit M of *Rhodopseudomonas viridis* at H200. Therefore, we propose that the transmembrane region 11 and the histidine in the middle of this region will play an important role in the coordination of P700.

We hope that the suggestions outlined above will open the way to new molecular biological experiments, including mutation experiments of the large subunits A and B. However, we must stress that only an electron density map calculated at higher resolution will be able to confirm our analyses. Such a map, incorporating new medium resolution data, is presently in preparation and will hopefully be available in the near future.

Acknowledgements

We thank H.T Witt and W. Saenger for helpful discussions and careful reading of the manuscript. This work was supported by the Deutsche Forschungsgemeinschaft through Sonderforschungsbereich 312 (H.T. Witt and W. Saenger) and by the Fonds der Chemischen Industrie (W. Saenger, H.T. Witt).

References

[1] Deisenhofer, J., Epp, O., Miki, K., Huber, R. and Michel, H. (1985) Nature 318, 618–624.
[2] Feher, G., Allen, J.P., Okamura, M.Y. and Rees, D.C. (1989) Nature 339, 111–116.
[3] Golbeck, J.H. (1992) Annu. Rev. Plant Mol. Biol. 43, 293–324.
[4] Sonoike, K., Hatanaka, H. and Katoh, S. (1992) Research in Photosynthesis I.4 (Proc. IX Int. Cong. Photosynthesis, Nagoya, Japan (Murata, N., ed.), pp. 605–608, Kluwer, Dordrecht.
[5] Mühlenhoff, U., Haehnel, W; Witt, H.T. and Herrmann, R.G. (1993) Gene 127, 71–78.
[6] Hladik, J. and Sofrova, D. (1991) Photosyn. Res. 29, 171–175.
[7] Shubin, V.V., Tsuprun, V.L., Bezsmertnaya, I.N., Karapetyan, N.V. (1993) FEBS Lett. 334, 79–82.
[8] Rögner, M., Mühlenhoff, U., Boekema, E.J. and Witt, H.T. (1990) Biochim. Biophys. Acta 1015, 415–424.
[9] Witt, I., Witt, H.T., Di Fiore, D., Rögner, M., Hinrichs, W., Saenger, W., Granzin, J., Betzel, C. and Dauter, Z. (1988) Ber Bunsenges. Phys. Chem. 92, 1503–1506.
[10] Witt, H.T., Krauß, N., Hinrichs, W., Witt, I., Fromme;P. Pritzkow, W. and Saenger, W. (1992) Research in Photosynthesis I (Proc. IX Int. Cong. Photosynthesis, Nagoya, Japan (Murata, N., ed.), pp. 521–528, Kluwer, Dordrecht.
[11] Krauss, N., Hinrichs, W., Witt, I., Fromme, P., Pritzkow, W., Dauter, Z., Betzel, C., Wilson, K.S., Witt, H.T. and Saenger, W. (1993) Nature 361, 326–331.
[12] Hippler, M., Ratajczak, R. and Haehnel, W. (1989) FEBS Lett. 250, 280–284.
[13] Chitnis, P.R., Purvis, D. and Nelson, N. (1991) J. Biol. Chem. 266, 20146–21151.
[14] Hatanaka, H., Sonoike, K., Hirano, M.,and Katoh, S. (1993) Biochim. Biophys. Acta 1141, 45–51.
[15] Collyer, C.A., Guss, J.M., Sugimura, Y., Yoshizaki, F. and Freeman, H.C. (1990) J. Mol. Biol. 211, 617–632.
[16] Tsukihara, T., Fukuyama, K., Nakamura, M., Katsube, Y., Tanaka, N., Kakudo, M., Wada, K., Hase, T. and Matsubara, H. (1981) J. Biochem. 90, 1763–1773.
[17] Otaka, E. and Ooi, T. (1989) J. Mol Evol. 29, 246–254.
[18] Moser, C.C., Keske, M., Warncke, K., Farid, R.S. and Dutton, P.L. (1992) Nature 335, 796–802.
[19] Otsuka, J., Miyachi, H. and Horimoto, K. (1992) Biochim. Biophys. Acta 1118, 194–210.
[20] Kirsch, W., Seyer, P. and Herrmann, R.G. (1986) Curr. Genet. 10; 8; 843–855.
[21] Fish, L.E., Kück, U. and Bogorad, L. (1985) J. Biol. Chem. 260, 1413–1421.
[22] Allen, J.P., Feher, G., Yeates, T.O., Komiya, H. and Rees, D.C. (1987) Proc. Natl. Acad. Sci. USA 84, 6162–6166.
[23] Webber, A.N. and Malkin, R. (1990) FEBS Lett. 264, 1–4.
[24] Smart, L.B., Warren;P.V., Golbeck, J.H. and McIntosh, L. (1993) Proc. Natl. Acad. Sci. USA 90, 1132–1136.
[25] Kyte, J. and Doolittle, R.F. (1982) J. Mol. Biol. 157, 105–132.
[26] Degli Esposti, M., Crimi, M. and Venturoli, G. (1990) Eur. J. Biochem. 190, 207–219.
[27] Mühlenhoff, U. (1991) Thesis, Technische Universität Berlin.